

Corrections

MEDICAL SCIENCES. For the article “Inhibitors of soluble epoxide hydrolase attenuate vascular smooth muscle cell proliferation,” by Benjamin B. Davis, David A. Thompson, Laura L. Howard, Christophe Morisseau, Bruce D. Hammock, and Robert H. Weiss, which appeared in number 4, February 19, 2002, of *Proc. Natl. Acad. Sci. USA* (**99**, 2222–2227; First Published February 12, 2002; 10.1073/pnas.261710799), due to a printer’s error, the footnote symbols in the author affiliations and one footnote appear incorrectly. The author line, the corrected affiliations, and the corrected footnote appear below.

**Benjamin B. Davis^{*††}, David A. Thompson^{*§¶},
Laura L. Howard^{*}, Christophe Morisseau[§],
Bruce D. Hammock^{§¶}, and Robert H. Weiss^{*¶||**††}**

^{*}Division of Nephrology, Department of Internal Medicine, [†]Cell and Developmental Biology Graduate Group, [§]Department of Entomology, and [¶]Cancer Research Center, University of California, Davis, CA 95616; and ^{**}Department of Veterans Affairs Northern California Health Care System, Mather, CA 95655

^{††}To whom reprint requests should be addressed at: Division of Nephrology, TB 136, Department of Internal Medicine, University of California, Davis, CA 95616. E-mail: rhweiss@ucdavis.edu.

www.pnas.org/cgi/doi/10.1073/pnas.082093899

NEUROBIOLOGY. For the article “Heteromultimers of DEG/ENaC subunits form H⁺-gated channels in mouse sensory neurons,” by Christopher J. Benson, Jinghie Xie, John A. Wemmie, Margaret P. Price, Jillian M. Henss, Michael J. Welsh, and Peter M. Snyder, which appeared in number 4, February 19, 2002, of *Proc. Natl. Acad. Sci. USA* (**99**, 2338–2343), the authors note that the author “Jinghie Xie” should be spelled “Jinghui Xie.” The online version of this article has been corrected.

www.pnas.org/cgi/doi/10.1073/pnas.082095399

EVOLUTION. For the article “The origin of the eukaryotic cell: A genomic investigation,” by Hyman Hartman and Alexei Fedorov, which appeared in number 3, February 5, 2002, of *Proc. Natl. Acad. Sci. USA* (**99**, 1420–1425; First Published January 22, 2002; 10.1073/pnas.032658599), the authors note that, on page 1421, the following sentence should be added at the end of the first paragraph of the *Materials and Methods*, and the reference below should be added to the reference list. “The Giardia database used in this paper is available at www.mbl.edu/Giardia. This database is described by McArthur *et al.* (24).”

1. McArthur, A. G., Morrison, H. G., Nixon, J. E., Passamaneck, N. Q., Kim, U., Hinkle, G., Crocker, M. K., Holder, M. E., Farr, R., Reich, C. I., *et al.* (2000) *FEMS Microbiol. Lett.* **189**, 271–273.

www.pnas.org/cgi/doi/10.1073/pnas.082070499

PSYCHOLOGY. For the article “Local and global attention are mapped retinotopically in human occipital cortex,” by Yuka Sasaki, Nouchine Hadjikhani, Bruce Fischl, Arthur K. Liu, Sean Marret, Anders M. Dale, and Roger B. H. Tootell, which appeared in number 4, February 13, 2001, of *Proc. Natl. Acad. Sci. USA* (**98**, 2077–2082), the author “Sean Marret” should be spelled “Sean Marrett.” The online version has been corrected.

www.pnas.org/cgi/doi/10.1073/pnas.062018699

Local and global attention are mapped retinotopically in human occipital cortex

Yuka Sasaki*, Nouchine Hadjikhani, Bruce Fischl, Arthur K. Liu, Sean Marrett, Anders M. Dale, and Roger B. H. Tootell

NMR Center, Department of Radiology, Massachusetts General Hospital, 149 13th Street, Charlestown, MA 02129

Edited by Marcus E. Raichle, Washington University School of Medicine, St. Louis, MO, and approved November 14, 2000 (received for review August 4, 2000)

Clinical evidence suggests that control mechanisms for local and global attention are lateralized in the temporal–parietal cortex. However, in the human occipital (visual) cortex, the evidence for lateralized local/global attention is controversial. To clarify this matter, we used functional MRI to map activity in the human occipital cortex, during local and global attention, with sustained visual fixation. Data were analyzed in a flattened cortical format, relative to maps of retinotopy and spatial frequency peak tuning. Neither local nor global attention was lateralized in the occipital cortex. Instead, local attention and global attention appear to be special cases of visual spatial attention, which are mapped consistently with the maps of retinotopy and spatial frequency tuning, in multiple visual cortical areas.

Clinical data suggest that in the temporal–parietal cortex, local attention and global attention are processed preferentially in opposing hemispheres (1, 2). According to one main model (3), attention to the local features of a visual scene preferentially involves neural control structures in the posterior superior temporal–parietal region in the left cortical hemisphere. Conversely, attention to the global aspects of a scene preferentially involves the corresponding temporal–parietal region in the opposite (right) hemisphere. Such lateralized mechanisms of local/global attention may be linked with mechanisms of parietal neglect and spatial attention—which also appear to be lateralized and located in the temporal–parietal cortex (3–5).

Recent positron-emission tomography (PET) studies tested this lateralized model of local/global attention. Initially, it was reported that attention to global features activated the right hemisphere, whereas attention to local features preferentially activated the left hemisphere (6), as in the prior clinical reports.

However, these lateralized PET foci were reported in occipital (visual) cortex, far posterior to the temporal–parietal region implicated in the clinical reports. Furthermore, subsequent PET studies in occipital cortex reported that (i) local/global attention is not lateralized (7), or (ii) it is lateralized but reversed relative to that reported earlier (i.e., highest in the left visual cortex for global attention, and highest in the right for local attention) (8). Thus, all logical possibilities (lateralized left–right, lateralized right–left, not lateralized) have been reported for local/global attention processing in occipital cortex—a confusing state of affairs.

One possible explanation involves eye movements. The two PET studies that reported lateralized activity were acquired during free viewing conditions; no attempt was made to control or measure where the eyes were looking at any time. Thus, the activity produced by each of the stimuli could also be localized more in the left or right hemisphere, depending on sensory variations based on where the subjects happened to look. A similar conclusion was reached by Mangun *et al.* (9).

The ultimate difficulty for any lateralized model of local/global attention is imposed by the architecture of the occipital cortical maps. It is now well established that visual spatial attention is mapped consistently with the cortical retinotopy (10–15), and the retinotopy itself is bilaterally symmetric; i.e., it

is not lateralized (11, 16–23). Thus it is difficult to imagine a model of occipital cortical organization in which local/global attention is lateralized, yet still mapped consistently with the retinotopy and spatial attention, which are not lateralized. As long as the eyes are free to stare directly at the object of attention (e.g., during normal viewing conditions or experimental fixation on a central target), a generalized model of retinotopic spatial attention would instead predict that (i) attention to local features would activate the foveal representation, in all of the retinotopic areas of occipital cortex, and (ii) attention to global features would activate more peripheral representations of the same cortical areas. To test these complementary predictions, we mapped the effects of local and global attention in occipital cortex with the use of functional MRI (fMRI).

Methods

Main Attention Task and Stimuli. The present experimental design was similar to that described earlier (11, 15). The main attention experiment was based on a block design, comprising 16 epochs per scan, and each epoch was 16 s long (see Fig. 1*b*). Eight normal subjects with (or corrected to) emmetropic vision either attended to the cued stimulus targets or passively viewed the same stimuli, in alternating epochs. The “attend” epochs were further subdivided into two conditions. In one condition, the subjects discriminated the global features of the stimulus set (“global” attention), whereas in the other condition, subjects discriminated the local features of the stimulus set (“local” attention).

The stimulus set comprised four stimuli, based on two arithmetic symbols (+ and ×), which were shown at both local and global scales (see Fig. 1*a*). The stimuli were presented in rapid succession, and the stimulus set remained equivalent throughout the experiment. During the “attend global” epochs, the subjects focused on whether the global shape of the stimulus was a + or a ×, with the use of a magnetic resonance (MR)-compatible response box. During the “attend local” epochs, the subjects instead focused on whether the stimulus was made up of individual ×’s or +’s.

During the main tests, the global figures subtended a visual angle of 29.4°, and the individual symbols subtended an angle of 2.4°. Subjects were instructed to steadily fixate the center of the stimulus throughout the experiment. The stimulus was designed so that the center of the global × and +, and the central local × and local + were all centered on the stimulus screen. Thus the center of the central local figure also served as a fixation point, without requiring a superimposed fixation target. Subjects did

This paper was submitted directly (Track II) to the PNAS office.

Abbreviations: MR, magnetic resonance; fMRI, functional MRI; PET, positron-emission tomography.

*To whom reprint requests should be addressed. E-mail: yuka@nmr.mgh.harvard.edu.

The publication costs of this article were defrayed in part by page charge payment. This article must therefore be hereby marked “advertisement” in accordance with 18 U.S.C. §1734 solely to indicate this fact.

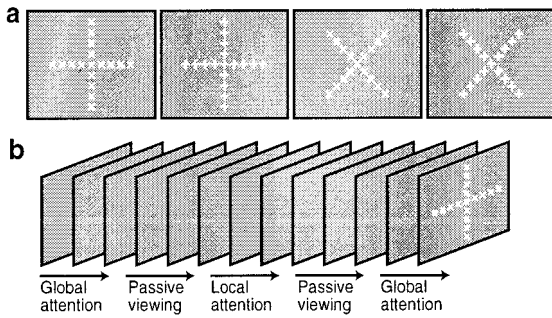


Fig. 1. Experimental stimuli and design. (a) The four stimuli, which were shown rapidly (≈ 2 Hz) throughout the main experiment, in randomized order. (b) A schematic diagram of that stimulus presentation over time.

not need to look elsewhere (i.e., to break fixation) to optimally resolve any of the local or global targets.

At the start of each epoch, subjects were briefly cued (300-ms color change) to (i) attend locally, (ii) attend globally, or (iii) passively view the stimuli. Throughout each attend epoch, each of the four stimuli was presented until the subject made a response decision via the button box. Thus, each stimulus remained visible until the subject responded (in practice, approximately 500 ms). To minimize retinal aftereffects, a stimulus mask (comprising all four stimuli, superimposed) was presented for 80 ms immediately after every stimulus presentation. Then the next local/global stimulus was presented immediately after the mask, and so on. During the following “passive viewing” epoch, the exact stimulus presentation rate and schedule (recorded from the immediately preceding attend epoch) was duplicated.

Before any scanning, each subject was well trained on the task outside the magnet, so that performance stabilized before data collection. Within the scanner, subjects performed this task during 8–14 scans (16,384–28,672 images) within a given scan session. Feedback about performance accuracy was given to the subject after each scan, to boost motivation and improve performance. Subjects frequently were reminded to maintain fixation on the central point and to respond as quickly as possible.

Retinotopic Control Stimuli I: Phase-Encoded Mapping. To confirm the retinotopic location of the attention targets and to reveal the borders of the retinotopic visual areas, we also acquired phase-encoded retinotopic maps from each subject, based on 64-s stimulus cycles, in additional scan sessions (11, 16–24).

Control Stimuli II: Spatial Frequency Peak Tuning. In additional control scans, we tested for an organization of peak spatial frequency tuning. This test used phase-encoded stimuli (achromatic sinusoidal gratings), and the spatial frequency was varied systematically from 0.05 to 2.0 cycles per degree within each 64-s cycle. The gratings were presented in contrast counterphase (2.5 Hz), with the phase changed randomly every 400 ms. The gratings were presented over the whole extent of the stimulus screen ($48^\circ \times 36^\circ$ of visual angle), and a central fixation spot was always present. These data were analyzed by Fourier-based phase-encoded approaches (11, 16–24).

Control Stimuli III: Local/Global Attention Task at a Different Spatial Scale. In additional scans, we attempted to determine whether variations in the overall size (“scale”) of the local/global stimuli would produce any effects (e.g., lateralization) that are not predicted by the retinotopy. Because the stimulus extent was already quite large in the standard experiments ($\approx 30^\circ$ diameter), we varied the scale of the local/global attention targets by

making them both smaller, moving the visual display screen further away from the subject, and ensuring that it remained emmetropic for each subject. At this reduced stimulus size, the global stimulus subtended a visual angle of 11.4° , and each local feature subtended an angle of 0.9° .

Eye Movement Recordings. Eye movements were measured while several of the subjects were performing the main attention experiments, with the use of MR-compatible goggles (Ober2; Permobil Meditech AB, Timre, Sweden), at a sampling rate of 250 Hz.

Imaging Procedures. Imaging procedures were as described (11, 15, 20, 22, 23). All subjects were scanned in a 3-T scanner with EPI. MR images were acquired with the use of a custom-built, quadrature-based, semicylindrical surface coil, and voxels that were 3.1 mm^2 in area in plane and 3–4 mm in thickness. Altogether, 81 scans (165,888 images) were acquired for our main attention task (see below). Head motion was minimized by using bite bars with deep, individually molded dental impressions. These experiments were covered by Massachusetts General Hospital Human Studies protocol 96-7464.

Data Analysis. The visual areas analyzed here, and the stimuli used to define them, are described elsewhere: V1, V2, V3/VP (11, 16–23, 25, 26), V3A (11), V4v (16, 17, 19, 20), V7 (11, 21), V8 (20), and MT+ (26–33). [The flattened cortical software we used (34–36) is freely available at <http://www.nmr.mgh.harvard.edu/freesurfer>.] Additions to this cortical flattening approach include (i) sampling of phase-encoded values of either retinotopic eccentricity or spatial frequency peak tuning, in one-dimensional lines across the cortical surface, and (ii) group-averaged fMRI data from all eight subjects, in a common morphed flattened map (35).

Results

Local Versus Global Attention. In general, subject performance on the attention task was excellent. During local versus global attention conditions, there were no significant differences in the average accuracy (97.4% vs. 97.0%, respectively, $t = 1.34$, $df = 7$, not significant) or latency (538 ms vs. 552 ms, respectively, $t = 1.49$, $df = 7$, not significant). These values are consistent with the maintenance of a moderate (and statistically equivalent) attentional load, during both the local and global attention conditions.

This experiment was designed so that subjects could perform the task while maintaining fixation on the center of the central \times or $+$. Unlike studies requiring central fixation during covert attention to a peripheral target, fixation in the present task was relatively easy to maintain, because the central fixation target coincided with the center of the attention target(s). Nevertheless, to confirm this presumptive fixation stability, eye movements were measured from subjects while they were in the magnet, monitoring the stimuli and performing the discrimination task. Such tests confirmed that subjects maintained stable fixation on the central fixation point while performing the experimental task (see Fig. 2a). There was much greater variation in eye position when the same subject was instead instructed to view the stimuli freely (Fig. 2b), as in some previous PET studies on local/global attention. In such free viewing conditions, the location of the attention targets projects to varying cortical locations, and to either hemisphere, in an uncontrolled manner.

Fig. 3a shows the main experimental comparison between the effects of local versus global attention, in one representative subject. One main hypothesis was that during the attend local epochs, MR activity would be highest in the cortical representation of the most central \times or $+$ (i.e., throughout the representation of 0 – 1.2° of eccentricity)—because subjects attended

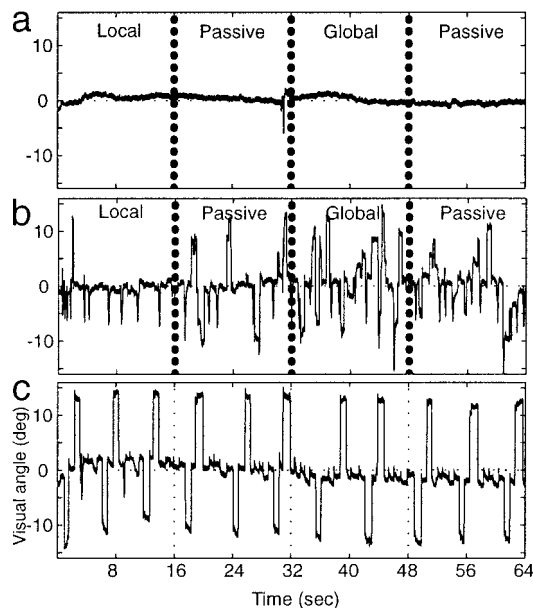


Fig. 2. Central fixation furnished retinotopic stimulus control. Eye movements recorded from one subject in the scanner, during the main attention task and control conditions are shown. Each panel shows eye movements recorded along the horizontal axis of the visual field. (a and b) The recordings were made during a portion of the main attention task (e.g., Fig. 1), including one block of local and global attention, and two blocks of passive viewing. (a) The subject was instructed to maintain central fixation while performing the task, as in all of our main experiments. (b) Eye movements acquired when this subject was instructed instead to view the stimuli freely while performing the task. (c) A calibration recording, in which the subject was instructed to systematically shift his or her gaze to each of the four peripheral extremes in the global stimulus.

to the most central local figure in our local attention task. From a comparison of the relative activity maps produced by local attention (e.g., blue-cyan in Fig. 3a and d) with the retinotopic representation of foveal eccentricities (e.g., red in Fig. 3b), it is clear that this hypothesis was confirmed.

A second (and complementary) hypothesis was that during the attend global epochs, the elevated MR activity should instead extend much further across the cortex, consistent with the representation of the much more peripheral visual field extent of the global \times and $+$. In the main experiment, the global \times and $+$ extended to $\sim 15^\circ$ eccentricity in the visual field. Therefore, the activity related to global attention (yellow-red in Fig. 3a) should extend to the corresponding cortical representation of $\sim 15^\circ$ eccentricity (within the green pseudocolor in Fig. 3b) and not beyond it. Our data also confirmed this second hypothesis in all subjects (Fig. 3d).

The relative MR activity produced by global attention tended to be lower in amplitude and topographically more scattered, compared with that produced by local attention (Fig. 3a). This result is actually predicted by the retinotopy of the attention targets and by models of spatial attention as a “zoom lens” (37), but additional factors may also contribute.

The results illustrated in Fig. 3 were quite consistent, both within and across subjects. For instance, Fig. 3d shows the activity maps during local/global attention, when averaged across all eight subjects. In all cases, attention to the local features of the stimulus (central \times or $+$) activated the foveal representation of cortex, and attention to the global features of the same stimulus produced relatively higher activity in the more peripheral representations. Control analysis (using subtractions against the passive viewing conditions) confirmed that these MR

effects reflected an increase in the expected cortical representations during the appropriate (local or global) attention condition, rather than a decrease during the converse conditions.

Thus, activity due to local and global attention was mapped consistently with the retinotopic projection of the stimuli. As in previous fMRI studies of visual spatial attention, the local/global increases occurred in the retinotopically appropriate cortical representations. These effects were most prominent in extrastriate areas such as V2, V3/VP, V3A, and V4v (see Fig. 3a and d), but such effects also could be seen in V1 in some subjects. This finding supports the hypothesis that local attention and global attention are simply special cases of visual spatial attention, at least in these retinotopic areas.

It was less clear whether more anterior visual areas (e.g., V7, V8, MT+) were preferentially activated by local or global attention. However, the decreased effect in these anterior areas may reflect technical factors rather than fundamental biological properties. In these higher-order areas, the receptive field sizes [and the corresponding retinotopic point-spread functions (11, 19)] are presumably larger than those in lower-tier areas such as V1. Therefore the lack of local/global attention differences in V8 and MT+ could result simply from the extensive retinotopic overlap of foveal and peripheral representations in these areas. In addition, the lack of color or motion in the attention targets may have triggered little corresponding effect in areas such as V8 or MT+ (respectively).

A priori, one might expect that the effects of local vs. global attention would cancel in the foveal representation, because of retinotopic overlap. Because the foveal representation is part of the global attention target as well as the local attention target, attention to this same foveal representation in both conditions might well produce no net difference in activity. Evidently (see Fig. 3a and d), the effects of local attention instead outweighed the effects of the global attention, possibly because attention was spatially more “concentrated” in the foveal representation during the local attention, compared with the global condition—consistent with the zoom lens model of spatial attention (37).

As one would expect from the retinotopy, these maps of local versus global attention activity appeared to be bilaterally balanced. To test the validity of this observation more formally, we counted the number of vertices (roughly proportional to the number of voxels, but more appropriate for this flattened analysis) on the cortical surface, which were preferentially activated ($P < 0.01$) by either local or global attention, in left vs. right hemispheres, in each subject tested. Using a two-factor ANOVA (hemisphere \times local/global attention), we found no significant interactions between the two factors and no significant effect of either factor on the number of vertices (Fig. 4). The local/global attention conditions were also bilateral when tested at systematically higher statistical thresholds ($P < 0.001$ and 0.0001 ; see Fig. 4). Thus, neither local attention nor global attention was significantly lateralized in our task.

Spatial Frequency Sensitivity. In both psychophysical (38) and imaging (39) studies, attention to local and global features has been related to variations in spatial frequency sensitivity (see also ref. 40). The rationale is as follows. In each stimulus configuration, the global stimuli are always much larger than the local stimuli. Therefore, perhaps mechanisms of spatial frequency sensitivity are shared with mechanisms of attention to the larger and smaller targets discriminated in the global and local attention tasks, respectively.

This hypothesis is more complicated than it sounds. For one thing, the spatial frequency spectrum of the local and global features was largely overlapping—much more than one might expect from simply measuring the size of the two kinds of targets. Thus it is quantitatively difficult to suppose that the spatial frequency components required for local and global target

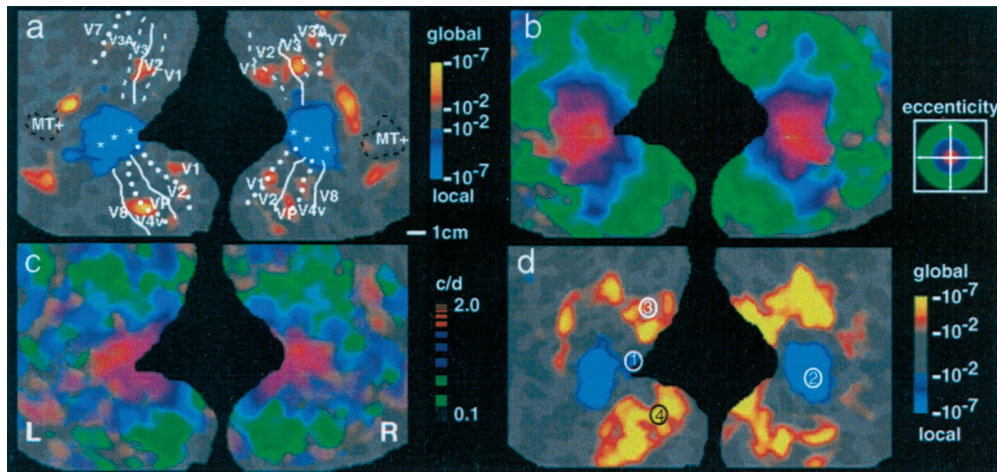


Fig. 3. Maps of local/global attention in comparison with maps of retinotopic eccentricity and spatial frequency peak tuning. Each panel shows flattened maps of the occipital cortex, including posterior portions of the temporal and parietal lobes as well. The right hemisphere is shown on the right side of each panel, and the left hemisphere is shown on the left of each panel. The gyral/sulcal topography in the original brain is also shown (light gray = gyri; darker gray = sulci) “beneath” the pseudocolor activity maps. (a) A scale bar for approximate cortical surface measurements (1 cm) is shown at the bottom right. (a–c) Separate activity maps from a single subject. Visual area borders for the subject shown in a–c are included in a. (a) A typical activity map of local versus global attention, produced by subtracting the average MR levels during local attention from the average MR levels during global attention. MR activity that was significantly higher during local attention is pseudocoded blue through cyan. Activity that was significantly higher during global attention is shown in red through yellow (see significance scale to the right of a: minimum = $P < 10^{-2}$; maximum = $P < 10^{-7}$). (b) A conventional phase-encoded map of retinotopic eccentricity. It was produced by presenting a ring of checks at systematically varied visual field eccentricities. As illustrated in the activity legend to the right of b, red pseudocolor reveals voxels that responded maximally when the stimulus was confined to foveal (central) eccentricities (center of red $\approx 1.7^\circ$). Blue and green indicate voxels responding maximally when the stimuli were confined to parafoveal and more peripheral eccentricities, respectively (center of blue $\approx 4.2^\circ$, center of green $\approx 11.3^\circ$). (c) A phase-encoded map of spatial frequency tuning. As illustrated in the activity legend to the right of c, red pseudocolor represents voxels that were maximally activated when the grating was of high spatial frequency (two cycles per degree), green represents voxels maximally activated when the grating was of low spatial frequency (≥ 0.05 cycle per degree), and blue represents voxels activated by intermediate spatial frequencies. (d) The group-averaged local/global attention maps. The averaged result is similar to the individual subject result (a), except that it is statistically more significant, indicating good across-subject reliability. For optimal comparability, the averaged activity map has been overlaid on the cortical surface from the subject shown in a–c. In addition, four numbered circles indicate the foci of maximal local/global attention activity, as taken from previous PET studies (see text).

detection stimulated different populations of neurons, even if partially segregated spatial frequency “channels” do exist in human visual cortex (41, 42).

Nevertheless, evidence suggests that spatial frequency sensitivity covaries with the retinotopic representation of eccentricity, at least in visual cortex (21, 43, 44). To the extent that variations in spatial frequency sensitivity covary with the retinotopy (which is not lateralized), it is difficult to assume that spatial frequency sensitivity is cortically lateralized, as proposed in some studies (45, 46).

To clarify these questions, we conducted additional fMRI experiments to map the sensitivity to spatial frequency throughout the visual cortex, in the same subjects who were tested for local/global attention and retinotopy. The results were unambiguous in all subjects tested.

First, these additional fMRI experiments revealed systematic cortical maps of peak spatial frequency tuning. Such an architecture has not been revealed by human neuroimaging previously, except in preliminary form (21). The spatial frequency maps were qualitatively similar to each other, across most or all of the classical retinotopic areas (e.g., V1, V2, V3/VP, V3A, V4v, etc.). However, the maps were not quite identical in all of these cortical areas—notice the slight shift in peak spatial frequency tuning in the upper visual field representation (“lower” cortex), exactly at the border between V1 and V2 (white arrowhead in Fig. 5b). A similar shift in preferred spatial frequency tuning has been reported between V1 and V2 in monkeys (47) and cats (48).

Second, this organization of preferred spatial frequency was related to, but not identical with, the organization of retinotopic eccentricity (see Figs. 3b and c and 5). Voxels showing maximum fMRI responses to the higher spatial frequencies tested were

concentrated nearest the foveal representation. Correspondingly, sensitivity to progressively lower spatial frequencies was represented at more peripheral eccentricities. Thus like the retinotopy, the maps of spatial frequency sensitivity were bilaterally symmetrical rather than lateralized.

To quantify these topographic variations, we made one-dimensional plots of stimulus eccentricity and spatial frequency. Samples were made along lines of isopolar angle representations from V1 and averaged across upper and lower visual field representations, from left and right hemispheres, from multiple subjects. Consistent with many previous data (16–18, 24, 49), we found a near-logarithmic relationship between cortical distance and stimulus eccentricity, in accordance with the cortical magnification factor (Fig. 5c). Along the same sampling line, the preferred spatial frequency varied more linearly (Fig. 5d).

Variation in Spatial Scale. Of course, the sizes of the targets, which were defined as either local or global, depended on the size of the overall stimulus configuration. If our local and global attention effects were really a special case of spatial visual attention, then reducing the overall stimulus size (e.g., control stimulus 3; see *Methods*) should again have produced “center-surround” maps of local/global attention, respectively (Figs. 3 and 5). However, these activity patterns should be correspondingly smaller in the cortex, consistent with the smaller retinotopic representation of such stimuli. Quantitatively, local attention should produce an enhancement confined to the representation of the central $0\text{--}0.46^\circ$. Similarly, global attention should produce an enhancement extending to a retinotopic eccentricity of 5.7° —corresponding to the extent of the smaller global targets.

In all cases tested, the local/global attention maps produced

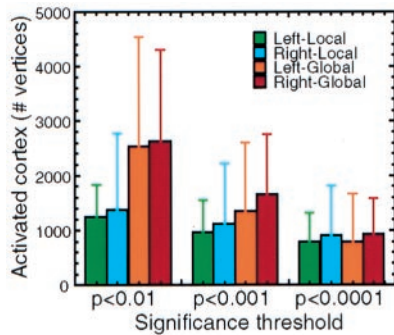


Fig. 4. Quantitative analysis across all subjects reveals no hemispheric lateralization of local/global attention. For each vertex in each (tessellated) cortical surface, fMRI activity was sampled preferentially from the middle and lower layers of the gray matter (e.g., refs. 16 and 34–36). This activity was added together to give a total number of activated vertices (y axis) for each of three different significance threshold levels (x axis). At all three levels, more cortical vertices were activated during global attention than during local attention, consistent with the greater cortical representation of the global attention target. However, there was no significant lateralization of local/global attention. The brackets above each bar represent one standard deviation.

by these smaller targets fit these predictions and were bilaterally symmetric. For instance, the average extent of the local attention activation (relative to the foveal centroid) had a mean of 16.2 (SD = 9.3) mm and 22.9 (SD = 9.0) mm, in the left and right hemispheres (respectively), from a set of hemispheres in which the subjects viewed the targets at the standard size (threshold level = $P < 0.01$). In the same set of hemispheres, targets viewed at the smaller size yielded correspondingly smaller extents of local attention activation (mean = 5.7 mm, SD = 4.2, and 7.6, SD = 5.1 mm, in the left and right hemispheres respectively), at the same significance threshold levels. ANOVA confirmed a strong effect of target size ($P < 0.0001$), but no significant difference between hemispheres, and no interaction between these factors.

Comparison with Previous PET Results. How can we reconcile our bilateral, retinotopic results with the previous reports of lateralized local/global activity in the occipital cortex? When interpreted differently, specific retinotopic features of those previous results were actually quite consistent with the results presented here.

First, let us assume that the neural substrates for lateralized local/global attention are not sensitive to the cognitive content of the attention targets, as indicated by clinical psychophysics (3, 50). This assumption of nonspecificity of stimulus content allowed us to compare the results from two previous PET studies that reported lateralized local/global activity, using either letters (6) or pictures (8) as targets, with our own results (in which arithmetic symbols were used).

This comparison is shown in Fig. 3*d*. Talairach coordinates (51) were used to colocalize the previous data relative to the present data. In both of the previous PET studies, the local attention task produced activity maxima near the occipital pole, where the foveal representation is located (see foci 1 and 2 in Fig. 3*d*). In contrast, the global attention task produced activity maxima that were located well outside the foveal representation but within the peripheral target representation (see foci 3 and 4)—just as we found in our study. Thus, if one disregards the lateralization reported previously, the retinotopic variation that we found also can be seen in previous studies.

Discussion

These experimental results were entirely consistent with the cortical retinotopy (16–20) and the associated retinotopy of spatial attention (10–15).

It might be argued that the center-surround (retinotopic) attention maps in this study were artifactual, because these experiments used constant fixation rather than normal (free) viewing. However, this center-surround prediction also holds true for the attentional activation produced during normal, free viewing. In fact, the center-surround prediction holds in any circumstance where the subjects are free to look directly at the object of their attention (as in the experiment here), and as long as the sensory aspects of the visual scene do not bias the brain activity to any specific region of the visual field (e.g., left or right hemifield).

The present attention results were also consistent with the functional organization of preferred spatial frequency, which is demonstrated here (e.g., Figs. 3*c* and 5). Attention to local features preferentially activated the foveal representation of cortex, where sensitivity to higher spatial frequencies was also highest. This finding is broadly consistent with the necessity to resolve finer visual features when attending to local targets of a scene. When attention is instead directed to the global features of the stimulus, it is unnecessary to resolve such fine details of the target, because the whole target is larger—which is consistent with the increased sensitivity to lower spatial frequencies at more peripheral eccentricities.

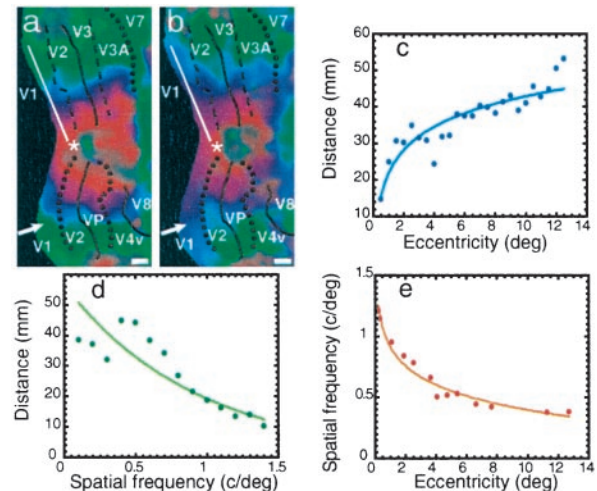


Fig. 5. Quantitative relationship between maps of spatial frequency peak tuning, compared with retinotopic eccentricity. Phase-encoded maps of retinotopic eccentricity and preferred spatial frequency from the right hemisphere of one subject are shown in *a* and *b*, respectively. In other respects, the map format is identical to that in Fig. 3*b* and *c*. As in Fig. 3*b* and *c*, the two maps are qualitatively similar, in that lines of iso-peak spatial frequency preference are organized roughly parallel to iso-eccentricity lines. The organizations are inversely related: higher spatial frequency preference occurs at decreased retinotopic eccentricity. The white arrowhead in *a* and *b* indicates a small but discrete shift in spatial frequency tuning between retinotopically matched regions of V1 and V2. To reveal the quantitative relationship between these two variables in a given retinotopically specific area, values for both dimensions were sampled along lines across the cortical surface, nearly parallel to the (iso-polar) horizontal meridian representation, within area V1 (e.g., white line in *a* and *b*), from the same subjects. Eight samples were averaged, with an equal number of samples from upper and lower visual field representations, and from right and left hemispheres. (*c* and *d*) These averaged values of retinotopic eccentricity (*c*) and the values of peak spatial frequency tuning (*d*), measured along the same lines. Cortical distances (shown on the y axis) were measured along this line, relative to the foveal representation (e.g., white asterisk in *a* and *b*). (*c*) The expected increase in cortical distance with progressive increases in stimulus eccentricity (16, 18, 24). In contrast, values of preferred spatial frequency tuning show a more monotonic decrease with increases in cortical distance from the foveal representation (e.g., white asterisk in *a* and *b*). (*e*) The direct relationship between preferred spatial frequency and retinotopic eccentricity.

Thus it may be an artificial distinction to ask whether local/global attention is mapped relative to the retinotopic map or, instead, to the spatial frequency map. Here these two maps work synergistically, so that local/global attention is mapped consistently with both the retinotopic and spatial frequency dimensions.

In this study, both local and global attention targets were centered in the visual field, and (by definition) the global targets were much larger than the local targets. This interaction raises an obvious question: what would happen if our local targets had instead been located in the peripheral visual field and attended covertly? Fortunately this general question has already been addressed in previous fMRI studies of spatial attention (10, 11, 13–15). The universal finding has been that covert attention to a small (e.g., local), peripherally located target produces MR enhancement at the corresponding retinotopic projection of the target, in all of the classically retinotopic areas, exactly as found here.

In this study we concentrated on resolving the issues of lateralization and retinotopy in the occipital cortex. Technically,

resolving these issues required an MR slice prescription that did not completely cover cortical regions anterior to the occipital cortex. Thus, we had incomplete coverage of the superior–posterior temporal–parietal region that was initially implicated in clinical studies on local/global attention. In this sense, our study was technically complementary to another fMRI study (52) that studied the temporal–parietal region but not the occipital region.

We thank Doug Greve for programming the experimental task and stimuli and for optimizing the across-subject averaging. We thank Moshe Bar for advice on the design of the stimulus mask. We thank Larry Wald, Mary Foley, and Bruce Rosen for MRI support; Tommy Vaughan for building the customized coil; and the Rowland Institute for machining MR-compatible hardware. These experiments were supported by a grant from the National Eye Institute (EY07980) (to R.B.H.T.). Y.S. was supported by a Fellowship from the Japan Society for the Promotion of Science. In addition, the contributing Human Brain Project/Neuroinformatics research (R01 NS39581 to A.M.D.) was funded jointly by the National Institute of Neurological Disorders and Stroke, the National Institute of Mental Health, and the National Cancer Institute.

1. Delis, D. C., Robertson, L. C. & Efron, R. (1986) *Neuropsychologia* **24**, 205–214.
2. Robertson, L., Lamb, M. & Knight, R. (1988) *J. Neurosci.* **8**, 3757–3769.
3. Robertson, L. C. & Lamb, M. R. (1991) *Cognit. Psychol.* **23**, 299–330.
4. Posner, M. I., Walker, J. A., Friedrich, F. J. & Rafal, R. D. (1984) *J. Neurosci.* **4**, 1863–1874.
5. Corbetta, M., Kincade, J. M., Ollinger, J. M., McAvoy, M. P. & Shulman, G. L. (2000) *Nat. Neurosci.* **3**, 292–297.
6. Fink, G. R., Halligan, P. W., Marshall, J. C., Frith, C. D., Frackowiak, R. S. & Dolan, R. J. (1996) *Nature (London)* **382**, 626–628.
7. Heinze, H. J., Hinrichs, H., Scholz, M., Burchert, W. & Mangun, G. R. (1998) *J. Cognit. Neurosci.* **10**, 485–498.
8. Fink, G. R., Marshall, J. C., Halligan, P. W., Frith, C. D., Frackowiak, R. S. & Dolan, R. J. (1997) *Proc. R. Soc. London Ser. B* **264**, 487–494.
9. Mangun, G. R., Heinze, H. J., Scholz, M. & Hinrichs, H. (2000) *J. Cognit. Neurosci.* **12**, 357–359.
10. Martinez, A., Anillo-Vento, L., Sereno, M. I., Frank, L. R., Buxton, R. B., Dubowitz, D. J., Wong, E. C., Hinrichs, H., Heinze, H. J. & Hillyard, S. A. (1999) *Nat. Neurosci.* **2**, 364–369.
11. Tootell, R. B., Hadjikhani, N., Hall, E. K., Marrett, S., Vanduffel, W., Vaughan, J. T. & Dale, A. M. (1998) *Neuron* **21**, 1409–1422.
12. Watanabe, T., Sasaki, Y., Miyachi, S., Putz, B., Fujimaki, N., Nielsen, M., Takino, R. & Miyakawa, S. (1998) *J. Neurophysiol.* **79**, 2218–2221.
13. Brefczynski, J. & DeYoe, E. (1999) *Nat. Neurosci.* **2**, 370–374.
14. Gandhi, S., Heeger, D. & Boynton, G. (1999) *Proc. Natl. Acad. Sci. USA* **96**, 3314–3319.
15. Somers, D. C., Dale, A. M., Seiffert, A. E. & Tootell, R. B. (1999) *Proc. Natl. Acad. Sci. USA* **96**, 1663–1668.
16. Sereno, M., Dale, A. M., Reppas, J. B., Kwong, K. K., Belliveau, J. W., Brady, T. J., Rosen, B. R. & Tootell, R. (1995) *Science* **268**, 889–893.
17. DeYoe, E., Carman, G., Bandettini, P., Glickman, S., Wieser, J., Cox, R., Miller, D. & Neitz, J. (1996) *Proc. Natl. Acad. Sci. USA* **93**, 2382–2386.
18. Engel, S. A., Glover, G. H. & Wandell, B. A. (1997) *Cereb. Cortex* **7**, 181–192.
19. Tootell, R., Mendola, J., Hadjikhani, N., Ledden, P., Liu, A., Reppas, J., Sereno, M. & Dale, A. (1997) *J. Neurosci.* **17**, 7060–7078.
20. Hadjikhani, N., Liu, A. K., Dale, A. M., Cavanagh, P. & Tootell, R. B. (1998) *Nat. Neurosci.* **1**, 235–241.
21. Tootell, R., Hadjikhani, N., Mendola, J., Marrett, S. & Dale, A. (1998) *Trends Cognit. Sci.* **2**, 174–183.
22. Tootell, R. B., Hadjikhani, N. K., Vanduffel, W., Liu, A. K., Mendola, J. D., Sereno, M. I. & Dale, A. M. (1998) *Proc. Natl. Acad. Sci. USA* **95**, 811–817.
23. Tootell, R. B., Mendola, J. D., Hadjikhani, N. K., Liu, A. K. & Dale, A. M. (1998) *Proc. Natl. Acad. Sci. USA* **95**, 818–824.
24. Engel, S. A., Rumelhart, D. E., Wandell, B. A., Lee, A. T., Glover, G. H., Chichilnisky, E. J. & Shadlen, M. N. (1994) *Nature (London)* **369**, 525.
25. Schneider, W., Noll, D. & Cohen, J. (1993) *Nature (London)* **365**, 150–153.
26. Beauchamp, M. S., Cox, R. W. & DeYoe, E. A. (1997) *J. Neurophysiol.* **78**, 516–520.
27. Tootell, R. B., Reppas, J. B., Dale, A. M., Look, R. B., Sereno, M. I., Malach, R., Brady, T. J. & Rosen, B. R. (1995) *Nature (London)* **375**, 139–141.
28. Tootell, R. B., Reppas, J. B., Kwong, K. K., Malach, R., Born, R. T., Brady, T. J., Rosen, B. R. & Belliveau, J. W. (1995) *J. Neurosci.* **15**, 3215–3230.
29. Lueck, C. J., Zeki, S., Friston, K. J., Deiber, M. P., Cope, P., Cunningham, V. J., Lammertsma, A. A., Kennard, C. & Frackowiak, R. S. (1989) *Nature (London)* **340**, 386–389.
30. Zeki, S., Watson, J. D., Lueck, C. J., Friston, K. J., Kennard, C. & Frackowiak, R. S. (1991) *J. Neurosci.* **11**, 641–649.
31. Watson, J. D., Myers, R., Frackowiak, R. S., Hajnal, J. V., Woods, R. P., Mazziotta, J. C., Shipp, S. & Zeki, S. (1993) *Cereb. Cortex* **3**, 79–94.
32. Dupont, P., Orban, G. A., De Bruyn, B., Verbruggen, A. & Mortelmans, L. (1994) *J. Neurophysiol.* **72**, 1420–1424.
33. McCarthy, G., Spicer, M., Adrignolo, A., Luby, M., Gore, J. & Allison, T. (1995) *Hum. Brain Mapp.* **2**, 234–243.
34. Dale, A. M., Fischl, B. & Sereno, M. I. (1999) *Neuroimage* **9**, 179–194.
35. Fischl, B., Sereno, M. I., Tootell, R. B. H. & Dale, A. M. (1999) *Hum. Brain Mapp.* **8**, 272–284.
36. Fischl, B., Sereno, M. I. & Dale, A. M. (1999) *Neuroimage* **9**, 195–207.
37. Eriksen, C. W. & St. James, J. D. (1986) *Percept. Psychophys.* **40**, 225–240.
38. Shulman, G. L. & Wilson, J. (1987) *Perception* **16**, 89–101.
39. Fink, G. R., Marshall, J. C., Halligan, P. W. & Dolan, R. J. (1999) *Neuropsychologia* **37**, 31–40.
40. Martinez, A. (1999) Ph.D. thesis (University of California, San Diego).
41. Georgeson, M. A. & Sullivan, G. D. (1975) *J. Physiol. (London)* **252**, 627–656.
42. Bodis-Wollner, I. & Hendley, C. D. (1979) *J. Physiol. (London)* **291**, 251–263.
43. Virsu, V. & Rovamo, J. (1979) *Exp. Brain Res.* **37**, 475–494.
44. Shulman, G. L. & Wilson, J. (1987) *Perception* **16**, 103–111.
45. Christman, S., Kitterle, F. L. & Hellige, J. (1991) *Brain Cognit.* **16**, 62–73.
46. Proverbio, A. M., Zani, A. & Avella, C. (1997) *Brain Cognit.* **34**, 311–320.
47. Foster, K. H., Gaska, J. P., Nagler, M. & Pollen, D. A. (1985) *J. Physiol. (London)* **365**, 331–363.
48. Movshon, J. A., Thompson, I. D. & Tolhurst, D. J. (1978) *J. Physiol. (London)* **283**, 101–120.
49. Hubel, D. H. & Wiesel, T. N. (1974) *J. Comp. Neurol.* **158**, 295–305.
50. Halligan, P. W. & Marshall, J. C. (1994) *Cognit. Neuropsychol.* **11**, 167–206.
51. Talairach, J. & Tournoux, X. (1988) *Co-Planar Stereotaxic Atlas of the Human Brain* (Thieme, New York).
52. Martinez, A., Moses, P., Frank, L., Buxton, R., Wong, E. & Stiles, J. (1997) *NeuroReport* **8**, 1685–1689.